Edited by H. Ryssel, P. Pichler - September 1995

Numerical Analysis of Hot-Electron Effects in GaAs MESFETs

Y. A. Tkachenko[a], C. J. Wei[a], J. C. M. Hwang[a], D. M. Hwang[b]

[a]Lehigh University, 19 Memorial Dr W, Bethlehem PA 18015, USA
[b]Motorola, APRDL, 3501 Ed Bluestein Blvd., Austin TX 78721, USA

Abstract

For the first time, numerical simulation of GaAs metal-semiconductor field-effect transistors subjected to hot-electron-induced degradation was performed. Experimentally observed open-channel current reduction and gate-drain field relaxation were verified. Maximum electric field which governs hot-carrier phenomena was found to depend on *Vdg* and not on *Vds*, as in the case of Si MOSFET. Extended surface depletion as a result of traps observed by high-voltage electron-beam-induced current imaging agreed well with *Nt* of 5×10^{12} and *Lt* of 0.1 μ used in simulation.

1. Introduction

It is well-known that hot electrons can be trapped in the gate oxide of a Si MOSFET causing its threshold voltage to shift. For a GaAs MESFET, hot electrons can also be trapped in the silicon nitride beside the gate (Fig. 1), causing the MESFET's transconductance to decrease without affecting its threshold voltage (Fig. 2). The hot electrons are generated by biasing the MESFET with high drain-source voltage (*Vds*) and RF driving it beyond pinch-off. Frequently confused with other gradual degradation effects, this phenomenon has not been reported until recently [1], [2]. In [2], we observed that hot-electron effects in MESFETs are mainly dependent on the peak drain-gate voltage (*Vdg*). In this paper, we analyze numerically hot-electron effects in MESFETs. Similarities and differences with hot-electron effects in MOSFETs are discussed. Direct experimental verification of the spatial distribution of hot-electron-induced traps is also presented.

2. GaAs MESFET simulation

Our analysis is based on 2-dimensional numerical simulation [3] of a MESFET. The MESFET consists of a 0.5 μ gate centrally located within a 3 μ source-drain spacing. The combined build-in charge density in SiN as well as at the SiN/GaAs interface, *Ni*, is assumed to be $1 \times 10^{12}/cm^2$. Hot-electron-induced traps are characterized by a sheet density of *Nt* spread over a length of *Lt* from the gate toward the drain (Fig. 1). This results in an enlarged surface depletion on the drain side of the gate, as shown in Fig. 3. The amount of trap-induced channel charge depletion is proportional to *Nt* (Fig. 4). The MESFET channel shrinks, hence the channel current decreases, in agreement with experimental data, as shown in Fig. 5. The resulting distribution of the electric field when simulated with *Vds* = 0 is also nonsymmetrical. As shown in Fig. 6, the maximum field *Em* is reduced on the drain side by the traps. Since hot-electron effects are critically dependent on *Em*, it was simulated under various bias conditions and trap densities. The simulation shows that,

unlike in a MOSFET, *Em* in a MESFET is proportional to $\sqrt{Vdg}$ instead of *Vds* (Fig. 7). This square root dependence can be derived by solving a 1D Poisson's equation with appropriate boundary conditions. Assuming that the surface states are uniformly distributed between gate and drain, whereas the traps are located only from 0 to *Lt* distance from the gate,

$$Em^2 = (q/\epsilon)Nd\{2Vdg - (q/\epsilon)[NsLdg^2 - 2NtLdgLt]\} \quad (1)$$

where q is electron charge; ϵ is dielectric constant; *Nd* is channel doping density; *Ns* is surface state density; and *Ldg* is gate-drain spacing. Fig. 8 shows that, based on 2D simulation, Em^2 decreases linearly with increasing density of traps, *Nt*, in agreement with (1).

3. Electric field relaxation in the degraded MESFET.

The above simulation agrees with the experimentally observed dependence on *Vdg* and the tendency for hot-electron-induced degradation to gradually saturate. Figure 9 shows that the reverse gate current, which is also caused by hot electrons, is proportional to exp(-1/*Vdg*). Figure 10 shows that, after the MESFET undergoes hot-electron stressing, the reverse gate current decreases uniformly across the typical operating range of *Vdg*. Figure 11 shows that, as measured by fractional changes in the open-channel current (*Imax*), the rate of hot-electron-induced degradation is approximately proportional to the square root of time.

4. High-voltage electron-beam-induced-current imaging.

The distribution of hot-electron-induced traps was directly verified using a novel high-voltage electron-beam-induced-current imaging technique [4]. By connecting the source and drain together, a Schottky diode is built in with the gate such that the induced current is proportional to the depletion depth by the surface states. As shown in Fig. 12, due to hot-electron-induced traps, the depletion region extends farther at the drain side of the gate (0.29 ± 0.04 μ) than at the source side of the gate (0.17 ± 0.04 μ). This is in agreement with $Lt = 0.1\ \mu$ used in the simulation.

Acknowledgement

This work was supported in part by the Air Force Wright Laboratory, Solid State Electronics Directorate, Microwave Division, under Contract No. F33615-90-C-1405.

References

[1] A. Watanabe, K. Fujimoto, M. Oda, T. Nakatsuka and A. Tamura, "Rapid degradation of WSi self-aligned gate GaAs MESFET by hot carrier effect", in *Proc. Int'l Reliability Physics Symp.*, 1992, pp. 127-130.

[2] Y. A. Tkachenko, Y. Lan, D. S. Whitefield, C. J. Wei, J. C. M. Hwang, L. Aucoin and S. Shanfield, "Accelerated dc screening of GaAs FETs for power slump tendency under RF overdrive," in *Dig. US Conf. GaAs Manufacturing Technology*, 1994, pp. 35-38.

[3] Silvaco International, Santa Clara, CA.

[4] D. M. Hwang, L. Dechiaro, M. C. Wang, P. S. D. Lin, C. E. Zah, S. Ovadia, T. P. Lee, D. Darby, Y. A. Tkachenko and J. C. M. Hwang, "High-voltage electron-beam-induced-current imaging of microdefects in laser diodes and MESFETs," in *Proc. Int'l Reliability Phys. Symp.*, 1994, pp. 470-477.

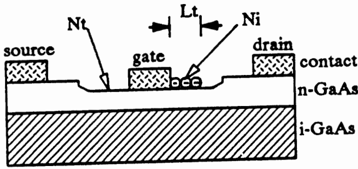

Fig. 1 MESFET structure indicating the distribution of hot-electron-induced traps.

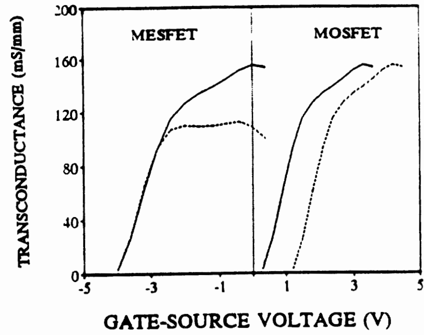

Fig. 2 Comparison of hot-electron effects of a MESFET and a MOSFET. (—) before, (---) after.

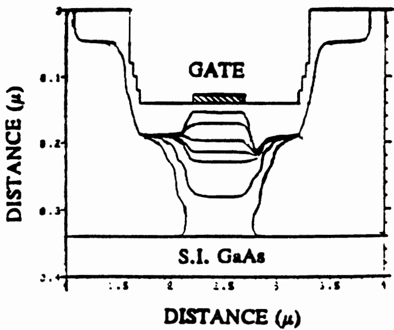

Fig. 3 Simulated depletion edge. Nt = $5\times10^{12}/cm^2$. Vds = 0. Vgs = 0.8, 0.6, 0.4, 0.2, 0, -1 and -3 top down.

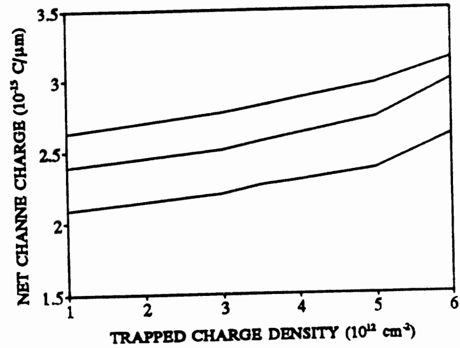

Fig. 4 Simulated net channel charge integrated on the drain side of the gate. Vds = 1 V. Vgs = -0.5, 0 and 0.5 V top down.

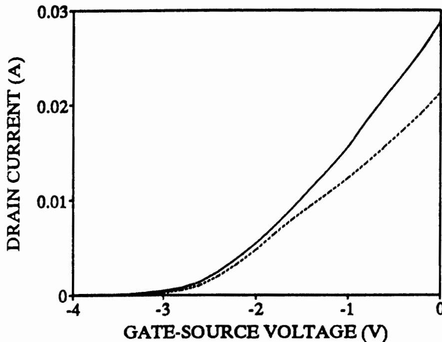

Fig. 5 Simulated transfer characteristics. (-) Nt = 0, (---) Nt = $5\times10^{12}/cm^2$. Vds = 0.6 V.

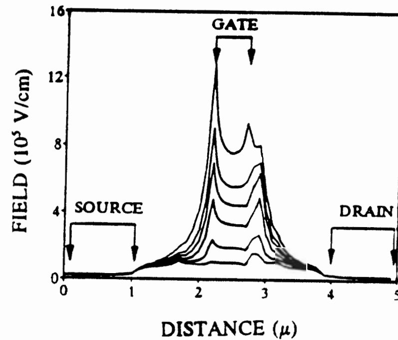

Fig. 6 Simulated electric field distribution. Vds = 0. Vdg = 1, 3, 7, 11, 15 and 23 V bottom up.

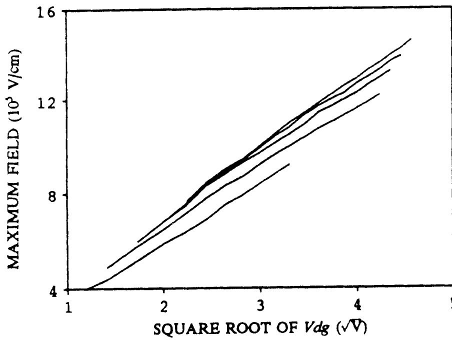

Fig. 7 Simulated maximum electric field. Vgs = -5, -4, -3, -2 and -1 V top down.

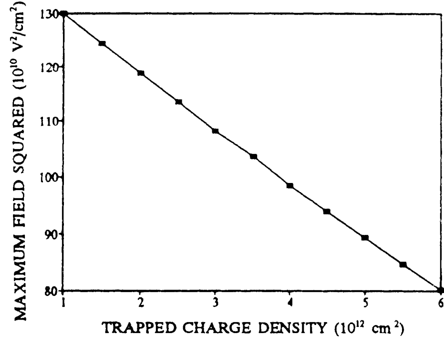

Fig. 8 Simulated maximum electric field. Vgs = -3 V, Vds = 13 V.

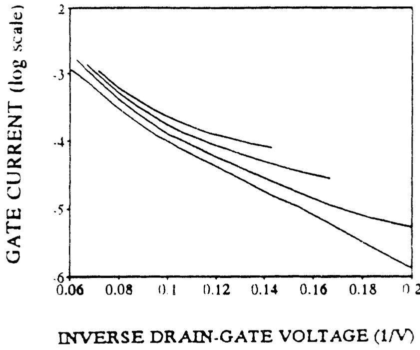

Fig. 9 Measured reverse gate current. Vgs = -4, -5, -6 and -7 V bottom up.

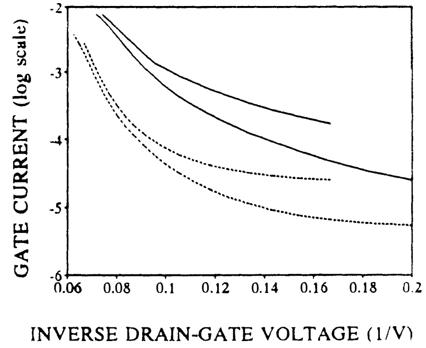

Fig. 10 Measured reverse gate current (—) before and (---) after. Vgs = -5 and -6 V bottom up.

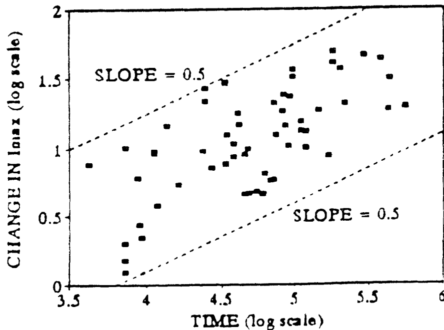

Fig. 11 Measured changes in MESFET drain current as a function of time.

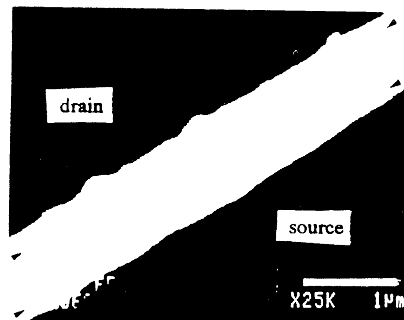

Fig. 12 High-voltage electron-beam-induced-current image of the MESFET of Fig. 1.